The Sensitivity of the African-Asian Monsoonal Climate to Orbital Parameter Changes for 9000 Years B.P. in a Low-Resolution General Circulation Model

J. E. KUTZBACH AND B. L. OTTO-BLIESNER

Center for Climatic Research and Department of Meteorology, University of Wisconsin, Madison 53706

(Manuscript received 1 September 1981, in final form 25 January 1982)

ABSTRACT

The earth's orbital parameters, precession, obliquity and eccentricity, produce solar radiation differences (compared to present) of ~7% at the solstices 9000 years before present (B.P.): more radiation in June-July-August, less in December-January-February. When this amplified seasonal cycle of solar radiation is used to drive a low-resolution general circulation model, an intensified monsoon circulation is simulated for Northern Hemisphere summer. The annual- and global-average land surface temperature and the annual- and global-average precipitation are the same for the simulated 9000 years B.P. climate and the present climate. Certain features of the simulated monsoon climate from this orbital-parameter sensitivity experiment agree with the paleoclimatic evidence.

1. Introduction

In a previous study, Kutzbach (1981) used a sensitivity experiment with a low-resolution general circulation model to test whether changes of solar radiation that were associated with changes of the Earth's orbital parameters could have caused the climatic changes of the early Holocene. The increased solar radiation of June-July-August 9000 years B.P. caused an intensified monsoon circulation over the African-Eurasian land mass; this feature of the simulated paleoclimate agreed with paleoclimatic observations (Kutzbach, 1981).

This study describes the simulated 9000 years B.P. climate in greater detail than the previous report and includes results for all seasons and the annual average. Kutzbach (1981) emphasizes two important elements of the experiment: 1) the solar radiation for 9000 years B.P. is ~7% more in July and ~7% less in January than at present; these changes are large, and they extend through tropical and middle latitudes of both hemispheres; 2) the annual-average solar radiation for 9000 years B.P. is close to the present value and this fact, coupled with an estimate that the thermal inertia of the ocean's mixed-layer effectively damps the seasonal response of the ocean temperature to the amplified solar radiation cycle, provides a basis for setting the ocean surface temperatures for 9000 years B.P. equal to present values. It then follows that the increased amplitude of the 9000 years B.P. seasonal solar radiation cycle causes increased heating of the land surface (which is mainly in the Northern Hemisphere) in June-July-August, and decreased heating in December-January-February. Because ocean surface temperatures remain at present values, land-ocean temperature contrasts are increased and intensified monsoonal circulations are the result.

Variations of the Earth's orbital parameters (obliquity, eccentricity and time of perihelion) are an important factor in the glacial-interglacial fluctuations of the past several hundred thousand years (Hays *et al.*, 1976; Imbrie and Imbrie, 1980). Most studies focus on the role of solar radiation changes at high or middle latitudes, an emphasis that is apparent in the pioneering work of Croll and Milankovitch [see Imbrie and Imbrie (1979) for an historical review; also Milankovitch (1941)]. Examples of studies with time-dependent climate models forced by solar radiation variations include Suarez and Held (1976, 1979) and Schneider and Thompson (1979).

A few authors emphasize that solar radiation changes at low latitudes might be important for understanding past climatic changes. Zeuner (1959) states that the precession of the equinox might provide an explanation for tropical pluvials, but he avoids speculating how the process might work. Bernard (1962) provides a detailed theoretical framework for the role of orbital parameter variations in producing climatic changes in the tropics. Much more recently, Prell (personal communication, 1981) suggests that the increased monsoon circulation and rains of the early Holocene are related to low-latitude solar radiation changes. Kutzbach (1981) and this report address this problem quantitatively with the aid of a general circulation model.

Section 2 describes the 9000 years B.P. solar radiation regime and summarizes the rationale for the

0022-4928/82/061177-12$07.00

use of modern surface boundary conditions in this sensitivity experiment. The characteristics of the low-resolution general circulation model used for the experiment and computational details are contained in Section 3. The simulated climate for 9000 years B.P. is described in Section 4; Section 5 compares the simulated climate for 9000 years B.P. with and without the North American ice sheet included as a boundary condition; Section 6 compares the results with paleoclimatic observations.

2. Solar radiation and lower boundary conditions

a. Solar radiation

Milankovitch (1941), Vernekar (1972), and, most recently, Berger (1978), have calculated the temporal and the latitudinal changes of solar radiation that are caused by changes of obliquity, time of perihelion and eccentricity. At 9000 years B.P., obliquity was 24.23° (the present value is 23.45°). The time of perihelion was 30 July (the present value is 3 January). Eccentricity was 0.01928 (the present value is 0.01676). Hopkins (1981, personal communication) develops algorithms that use Berger's astronomical solutions in order to calculate the seasonal radiation cycle for 9000 years B.P. on a daily basis; Hopkins' algorithms were used in the experiment reported by Kutzbach (1981) and in an early version of this study. The "calendar" used for calculating the solar radiation keeps the vernal equinox date as 21 March but allows other dates, such as the autumnal equinox date, to change as a function of the changing length of the astronomical seasons. Berger (1978) notes that the astronomical summer and winter half-years may differ in length by as much as 33 days, depending upon the eccentricity of the orbit and the time or location of perihelion. For example, the time interval between the vernal and autumnal equinox is 186.4 days at present but it was only 179.2 days at 9000 years B.P. (when perihelion was in July). As a result, identical calendar dates in different millenia may represent somewhat different portions of the seasonal solar cycle and this complicates comparisons.

An alternative to the calendar year is used in this study. A celestial year is defined in terms of 360° of celestial longitude, with $\lambda = 0$ at the vernal equinox (Berger, 1978). The common names for calendar months are applied to "celestial" months of increment $\Delta\lambda = 30°$. For example, the celestial month "April" refers to the average radiation (or average model output) for the interval from $\lambda = 10.16°$ to $\lambda = 40.16°$. The use of a celestial year assures that different millenia can be intercompared for identical portions ($\Delta\lambda$) of the seasonal solar cycle. The celestial year, however, doesn't explicitly allow for the varying length of time required for the earth to move through each 30° arc of celestial longitude. We have taken this factor into account in computing annual averages by weighting the solar radiation and the model results for each celestial month as a function of the time required to move each 30° increment. A detailed intercomparison of the calendar- and celestial-year approach to radiation and climate calculation is in preparation by J. Kutzbach and P. Guetter.

The model results for both calendar- and celestial-year calculations for 9000 years B.P. and the Present have been compared. The two simulations are qualitatively identical in that both develop intensified monsoon circulations; quantitatively, there are differences.

Table 1 summarizes the solar radiation by seasonal, annual, latitudinal, global and hemispheric averages. The 9000 years B.P. solar radiation increases in June-July-August and decreases in December-January-February by ~7% (compared to Present) across a broad latitudinal band; the absolute value of these differences is 25–35 W m^{-2} in the summer hemisphere. Because perihelion occurs near the summer solstice at 9000 years B.P. and near the winter solstice at Present, the differences (9000 years B.P. minus Present) in global-average and in tropical- and middle-latitude solar radiation are larger in June-July-August (JJA) and December-January-February (DJF) than in March-April-May (MAM) and September-October-November (SON).

The global- and annual-average solar radiation at 9000 years B.P. is very close to its present value (348 W m^{-2}; Table 1). Berger (1978) notes that changes of global- and annual-average solar radiation arise only from changes of eccentricity; using Berger's analytical expression, we find an increase of solar radiation at 9000 years B.P. of 0.005% compared to Present. The numerical calculations used in this study are not carried to the accuracy required to give this slight increase. Wetherald and Manabe (1975) conclude from general circulation model sensitivity experiments that changes of the solar constant of +2% result in changes of global- and annual-average surface temperature of ~ +3.0 K. Employing this sensitivity factor, the 0.005% increase of solar radiation would produce a global- and annual-average temperature increase of ~0.01 K for 9000 years B.P. (compared to Present).

The annual-average solar radiation at 9000 years B.P. is increased slightly at polar latitudes and decreased slightly at tropical latitudes, compared to Present (Table 1). The slight increase at polar latitudes may have contributed to the general high-latitude warming of polar regions during the early Holocene, but this topic is not pursued further in this report.

b. Lower boundary conditions

In contrast to the general circulation model experiments for glacial maximum conditions (18 000

TABLE 1. Latitudinal-, hemispheric- and global-average solar radiation (W m^{-2}) for seasons and annual average: 9000 years B.P. (9 K), Modern (M), 9000 years B.P. minus Modern (Δ), and percentage change (%).

	JJA				SON				DJF				MAM				Annual			
Latitude	9K	M	Δ	%	9K	M	Δ	%	9K	M	Δ	%	9K	M	Δ	%	9K	M	Δ	%
81.1°N	482	439	43	10	37	35	2	5	0	0	0	—	251	240	11	5	188	183	5	2.9
69.6	468	427	41	10	84	82	2	2	10	11	−1	—	285	277	8	3	208	204	4	1.9
58.0	477	440	37	8	157	156	1	1	59	68	−9	−12	336	331	5	2	253	252	1	.5
46.4	497	461	36	8	232	231	1	0	134	148	−14	−9	383	380	3	1	308	308	0	0
34.8	505	471	34	7	302	301	1	0	211	230	−19	−8	419	417	2	1	356	357	−1	−.1
23.2	497	465	32	7	361	360	1	0	285	308	−23	−7	439	439	0	0	393	394	−1	−.2
11.6	472	444	29	7	407	406	1	0	350	376	−26	−7	442	443	−1	0	417	418	−1	−.3
0	431	406	25	6	437	436	1	0	403	431	−28	−6	429	431	−2	−1	424	426	−1	−.3
11.6	374	354	20	6	450	449	1	0	441	470	−29	−6	398	402	−4	−1	417	418	−1	−.3
23.2	305	290	15	5	445	444	1	0	465	493	−28	−6	353	358	−5	−1	393	394	−1	−.2
34.8	226	217	9	4	425	423	2	0	472	499	−27	−5	294	300	−6	−2	356	357	−1	−.1
46.4	143	139	4	3	389	387	2	0	465	489	−24	−5	225	231	−6	−2	308	308	0	0
58.0	63	64	−1	−1	339	337	2	1	447	467	−20	−4	151	156	−5	−3	253	252	1	.5
69.6	11	11	0	—	286	283	3	1	438	453	−15	−3	80	84	−4	−4	208	204	4	1.9
81.1°S	0	0	0	—	250	247	3	1	451	465	−14	−3	35	36	−1	−4	188	183	5	2.9
Global	361	339	22	7	350	349	1	0	337	359	−22	−6	344	345	−1	0	348	348	0	0
N. Hemisphere	483	450	33	7	297	296	1	0	224	242	−18	−7	398	396	2	1	348	348	0	0
S. Hemisphere	239	228	11	5	404	402	2	0	451	477	−26	−5	290	294	−4	−1	348	348	0	0

years B.P.), where the lower boundary conditions differ greatly from present values and are specified from studies of the geologic record (Gates, 1976a,b; Manabe and Hahn, 1977; Williams *et al.*, 1974), the boundary conditions for 9000 years B.P. are set at present values. As described in Kutzbach (1981), the rationale for this simplification is twofold. First, this provides a clear test of the sensitivity of the model climate to the solar radiation changes. Second, the present boundary conditions may approximate the 9000 years B.P. boundary conditions, especially for the oceans.

Two lines of reasoning suggest that the ocean surface temperatures of 9000 years B.P. are close to present values. First, in the North Atlantic Ocean, where temperatures at 18 000 years B.P. are much lower than at present (CLIMAP, 1976), the major transition to interglacial and essentially modern conditions occurred by 9000 years B.P. (Ruddiman and McIntyre, 1973, 1981). We assume that the major post-glacial adjustments have also occurred in other parts of the world ocean by 9000 years B.P. Second, the 9000 years B.P. orbital parameters amplify the seasonal solar radiation cycle (compared to Present) but, as previously mentioned, they produce only small changes in global- and annual-average radiation; as a consequence the average change of surface temperature (land and ocean) could be as small as 0.01 K.

A large annual-average temperature change could only be caused by a strong covariance between the amplified radiation cycle and the seasonal cycle of albedo or mixed-layer depth. Schneider and Thompson (1979) use a zonal-average energy balance climate model with a mixed-layer ocean (represented by an appropriate thermal inertia) and with a present-day seasonal cycle of albedo to estimate the magnitude of this covariance effect. They find that a 25% increase in the amplitude of the seasonal cycle of solar radiation increases the global-average surface temperature by $\sim$0.32 K. Scaled to the 7% increase (relative to Present) in amplitude of the 9000 years B.P. radiation cycle, we can anticipate an increase of annual-average surface temperature of $\sim$0.09 K.

A rough estimate of the increased amplitude (δT) of the sea-surface seasonal temperature cycle in response to the increased amplitude (δQ) of the solar radiation cycle at 9000 years B.P. can be obtained by assuming that the entire increase (decrease) of radiation is used to increase (decrease) the temperature of the mixed-layer ocean with thermal inertia R, i.e., $R\,\delta T/\delta t = \delta Q(1 - \alpha)$. For a thermal inertia (R) corresponding to a mixed-layer depth of 100 m, for δQ = 20 W m^{-2}, and for a planetary albedo (α) of 0.30, the value of δT is $\sim$0.5 K.

These order-of-magnitude calculations of the expected seasonal and annual ocean surface temperature response to the modified seasonal solar radiation cycle, along with the previously mentioned paleoclimatic evidence, support the assumption that ocean surface temperatures are close to present values at 9000 years B.P. This assumption is understood to apply over large parts of the ocean; however, in certain areas, particularly near coasts where upwelling occurs, the 9000 years B.P. temperatures could depart significantly from modern values (Prell, 1981, personal communication).

In this initial study, land albedo and ground wetness for 9000 years B.P. are set at modern values although paleoclimatic evidence might suggest decreased albedo and increased wetness over tropical continents where raised lake-levels occur (Section 6). At 9000 years B.P. the Scandinavian ice sheet has disappeared but the North American ice sheet still extends across Canada from west of Hudson's Bay to the Atlantic coast (Bryson *et al.*, 1969). The omission of the Laurentide ice sheet from the lower boundary of the model results in an unrealistic simulation of the North American climate, but does not influence greatly the results for the African-Eurasian land mass that are emphasized in Section 4 (Section 5 compares experiments with and without the North American ice sheet). The 9000 years B.P. sea-ice extent is also set at modern values.

3. The low-resolution model

A low-resolution model of the general circulation of the global atmosphere is used for the experiment (Otto-Bliesner *et al.*, 1982). The model incorporates atmospheric dynamics based upon the equations of motion. The equations are formulated in spectral terms and the model retains longitudinal wavenumbers 1–10 and an 11.6° $\times$ 11.25° latitude-longitude grid for spectral-grid transforms. The model has five vertical levels and includes orographic influences of mountains (and ice sheets) as well as radiative and convective processes, condensation and evaporation. A surface heat budget is computed over land. The model requires that ocean surface temperature, land albedo, ground wetness, sea ice and ice sheet topography be specified. Ocean surface temperature and sea-ice are specified regionally from modern climatology, and they vary seasonally. Land albedo of snow-free regions is specified regionally from modern climatology at an annual-average value; ground wetness is a function of land albedo in these regions. Snow-on-land is specified latitudinally and seasonally from modern climatology. Cloudiness and empirical longwave radiative emissivities are specified latitudinally and seasonally from modern climatology for use in the radiation calculations.

The starting date for the 9000 years B.P. simulation is 1 April (λ = 10.16°) of "year 3" of a five-year model simulation of the modern climate (Otto-Bliesner *et al.*, 1982). In April 9000 years B.P. the

solar radiation is close to present values so that the simulated modern climate changes gradually to the simulated climate for 9000 years B.P. as the seasonal solar radiation cycle proceeds. The lower boundary conditions of ocean surface temperature, sea-ice and snow extent are changed daily, as the integration proceeds, according to a smoothed version of the present seasonal cycle that was fit to a 360-day year (or 360° of celestial longitude). The 9000 years B.P. simulation covers 14 months; it starts 1 April and finishes 1 June, 14 months later. The results for the first April and May are ignored, and the monthly, seasonal and annual averages for 9000 years B.P. are derived from the final 12-month period of the integration.

Because the extreme differences of solar radiation for low and middle latitudes are at the solstices (Table 1), the monsoon-related climatic differences between the 9000 years B.P. experiment and the modern (control) experiment are greatest around the solstices. We therefore emphasize the simulated climate of the two extreme seasons (JJA and DJF) and the two extreme months (July and January) of the 9000 years B.P. seasonal cycle.

Certain differences between the 9000 years B.P. experiment and the present (control) experiment are well above the noise level of the model. The noise level estimates are the standard deviations of climatic variables calculated for particular months, seasons or for the year, from a data set that was generated during a five-year seasonal cycle experiment (Otto-Bliesner *et al.*, 1982). Assuming that each year of the five-year experiment is equivalent to an independent experiment, a climatic difference (9000 years B.P. minus Present) is statistically significant as follows: at the 10% level if the difference equals 3 standard deviations, at the 5% level if the difference equals 4 standard deviations, and at the 1% level if the difference equals 6.5 standard deviations [*t*-test (see Chervin *et al.*, 1980)].

4. Results

The results are summarized as latitudinal, hemispheric and global averages, and depicted on charts for the African-Eurasian sector. Latitudinal averages are particularly appropriate for this sensitivity experiment because the differences of solar radiation between 9000 years B.P. and Present are functions of latitude. Charts are shown only for the African-Eurasian sector for two reasons: 1) the monsoon-like response to the amplified seasonal cycle of solar radiation of 9000 years B.P. is most apparent in the African-Eurasian sector because of the large latitudinal variation of the land-ocean distribution of the Eastern Hemisphere (land predominates from 70 to 23°N, ocean predominates south of 12°N); 2) the 9000 years B.P. climate in the North American sector is influenced by the Laurentide ice sheet, which is omitted from the boundary conditions in this sensitivity experiment (but see Section 5 for the results with the North American ice sheet included).

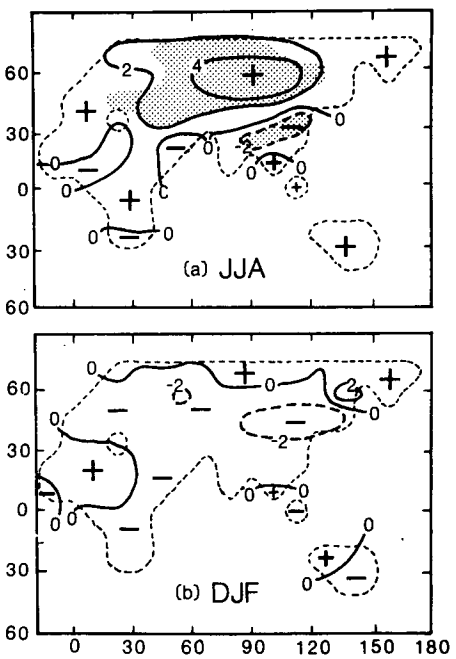

FIG. 1. Simulated land surface temperature (K) difference (9000 years B.P. minus Modern), for the sector 0–180°E: (a) JJA, (b) DJF. Grid points where the temperature differences exceed three standard deviations are indicated with shading. Temperature difference at ocean gridpoints is equal to zero (see text).

The description of the results involves comparisons between the simulated climate of 9000 years B.P. and the simulated present (control) climate. To avoid excessive repetition, we will omit references to the present (modern) standard of comparison; thus, for example, "higher temperature at 9000 years B.P." should be interpreted as "higher temperature at 9000 years B.P. compared to Present." Similarly, the term "difference" will always refer to 9000 years B.P. *minus* Present.

a. June-July-August

The increased solar radiation of JJA 9000 years B.P. causes higher surface temperatures across Eurasia (Fig. 1a). The temperature differences exceed 4 K over central Asia, and they exceed three standard deviations over an even larger area. The maximum increase is 5 K (five standard deviations) and occurs at 58°N, 90°E. The maximum temperature increase in July occurs at the same location but is 6 K, consistent with the maximum increase of solar radiation during that month. The magnitudes of these high-latitude temperature differences are similar to the results of Mason (1976) for a May-June 10 000 years B.P. experiment. The JJA 9000

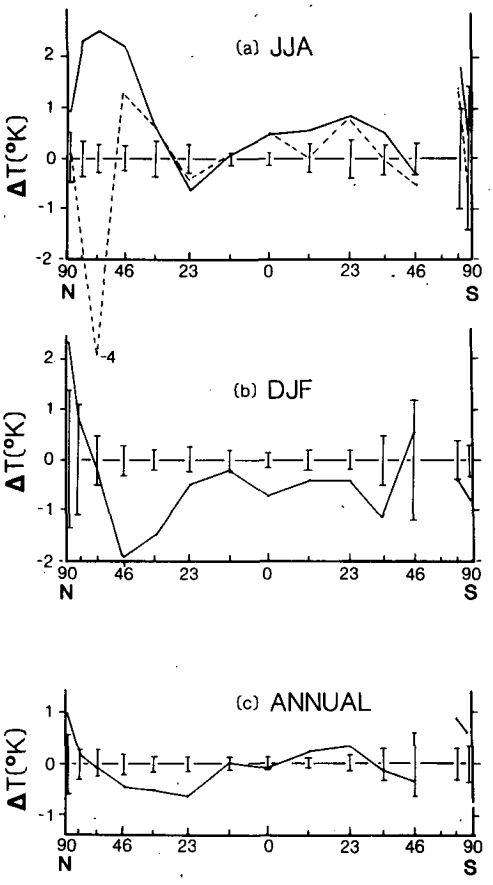

FIG. 2. Latitudinal average of simulated land surface temperature (K) difference ΔT (9000 years B.P. minus Modern), as function of sine of latitude. Positive values indicate warmer land surface temperature at 9000 years B.P. Vertical bars indicate one standard deviation about the modern average: (a) JJA, (b) DJF, (c) annual-average. There is only one land grid point at 46°S (South America) and no land grid point at 58°S. Temperature difference for case with North American ice sheet is indicated with dashed lines in (a).

years B.P. temperature is slightly lower than Present in portions of North Africa and especially in Southern Asia because cooler air is advected from the ocean and because the increased radiation is used to increase evaporation rather than to warm the surface; in contrast to the results at mid-latitude, the small decreases of temperature are generally of the same magnitude as the standard deviation and are therefore statistically significant at only a few locations in Southern Asia.

The latitudinal-average difference in land surface temperature for JJA 9000 years B.P. (Fig. 2a) exceeds 2.0 K and four standard deviations between 46 and 70°N. The JJA 9000 years B.P. surface temperature averaged over the Northern Hemisphere land is 1.2 K higher than Present (25.0°C versus 23.8°C; Table 2a). This difference exceeds 10 standard deviations.

In response to the increased heating and higher temperature of the African-Eurasian land surface, relative to the surrounding ocean that was kept at present temperature, there is a redistribution of atmospheric mass. The continent-wide monsoon low of JJA 9000 years B.P. (Fig. 3a) intensifies considerably compared to Present (Fig. 3b). The 900 mb geopotential height decreases at least 25 m across much of Eurasia (Fig. 3c), and the height differences inside this contour exceed 2 standard deviations. The 900 mb geopotential height at the center of the monsoon low (located at 35°N, 79°E for the simulated climate) is 710 m for JJA 9000 years B.P. compared to 762 m at Present, a decrease of 52 m (3 standard deviations). Over large parts of the ocean the 900 mb geopotential height increases.

The latitudinal-average (180°W–0–180°E) differences of 900 mb geopotential height for JJA (Fig. 4a) reflect the main features of the results for the African-Eurasian sector (0–180°E). Heights decrease to the north of 23°N; the heights decrease more over land than over ocean at most latitudes (Fig. 4b) and the land-ocean height difference exceeds 3 standard deviations between 23 and 46°N. This altered pressure distribution is associated with increased flow of air from ocean to land at low levels and leads to a general strengthening of the Northern Hemisphere summer monsoon circulation at 9000 years B.P.

The low-resolution general circulation model provides only limited information on the regional details of climate for 9000 years B.P. We summarize in schematic fashion those features of the intensified monsoonal circulation that are of highest statistical significance (Fig. 5). In JJA 9000 years B.P., strengthened low-level southerly and southwesterly winds carry moisture into West Africa and South Asia; this intensified circulation is consistent with the intensified low-level pressure distribution (Fig. 3a). Aloft, the tropical easterly jet stream is strengthened over the western Indian Ocean and equatorial Africa.

Detailed regional analyses of the sensitivity of the hydrological cycle to changes in the seasonal cycle of solar radiation are best deferred for experiments with high-resolution models. The low-resolution model used in this study simulates the areas of major precipitation of tropical and middle latitudes and their seasonal variations (Otto-Bliesner *et al.*, 1982), but the precipitation maxima delineating the ITCZ have elements with more north–south orientation than the observed narrow band and the monsoonal precipitation is not as well organized as the observed pattern. Global- and hemisphere-average precipitation and evaporation rates are comparable to (but somewhat larger than) observed rates; the model overestimates precipitation and evaporation rates over land but the difference, precipitation-minus-evaporation ($P - E$), is comparable to observations.

TABLE 2. Simulated surface temperature (a), precipitation (b) and precipitation-minus-evaporation (c); time averages are June-July-August (JJA), December-January-February (DJF), and Annual; space averages are Northern Hemisphere Land (NH, L), Southern Hemisphere Land (SH, L), and Global Average of Land and Ocean (G, L & O) for 9000 years B.P., Modern, Difference, Standard Deviation (σ), and statistical significance level of the Difference.

(a)

		Surface temperature				
Time average	Space average	9000 years B.P. (°C)	Modern (°C)	Difference (K)	σ (K)	Significance level (%)
JJA	NH, L	25.0	23.8	1.2	0.05	0.1
	SH, L	2.5	1.7	0.8	0.35	
	G, L & O	17.8	17.5	0.3	0.04	1
DJF	NH, L	1.0	1.7	−0.7	0.18	5
	SH, L	13.2	13.7	−0.5	0.11	5
	G, L & O	13.7	13.9	−0.2	0.04	5
Annual	NH, L	13.3	13.6	−0.3	0.08	
	SH, L	7.5	7.2	0.3	0.04	1
	G, L & O	15.9	15.9	0	0.02	

(b)

		Precipitation				
		9000 years B.P. (cm day^{-1})	Modern (cm day^{-1})	Difference (cm day^{-1}) (%)	σ (cm day^{-1})	Significance level (%)
JJA	NH, L	0.47	0.42	0.05 (13)	0.010	5
	G, L & O	0.35	0.35	0 (0)	0.001	
DJF	NH, L	0.32	0.36	−0.04 (−11)	0.008	5
	G, L & O	0.32	0.31	0.01 (3)	0.002	5
Annual	NH, L	0.38	0.37	0.01 (2)	0.004	
	G, L & O	0.33	0.33	0 (0)	0.001	

(c)

		Precipitation-minus-evaporation				
		9000 years B.P. (cm day^{-1})	Modern (cm day^{-1})	Difference (cm day^{-1})	σ (cm day^{-1})	Significance level (%)
JJA	NH, L	−0.10	−0.10	0	0.10	
	G, L & O	0	0	0	0.003	
DJF	NH, L	0.12	0.14	−0.02	0.01	
	G, L & O	0.02	0.02	0	0.002	
Annual	NH, L	0.02	0.02	0	0.006	
	G, L & O	0.01	0.01	0	0.002	

Over Northern Hemisphere land, the precipitation rate is 0.47 cm day^{-1} for JJA 9000 years B.P. and ~0.42 cm day^{-1} at Present, an increase of 13% (Table 2b); over the North African-Asian sector, the increase is 26% (Table 3). The $P - E$ rate is unchanged for Northern Hemisphere land (Table 2c) but is increased for the North African-Asian sector (Table 3). The latitudinal-average difference in land $P - E$ for JJA 9000 years B.P. compared to Present (Fig. 6a) is positive between 0 and 23°N; at 23°N the $P - E$ increase is 0.15 cm day^{-1} (135 mm for the summer season).

b. December-January-February

The decreased solar radiation of DJF 9000 years B.P. (Table 1) causes lower surface temperatures over many parts of Africa-Eurasia (Fig. 1b). Because model variability is relatively high in DJF (compared to JJA), the lower surface temperatures are not statistically significant. The largest temperature difference is −4 K (2 standard deviations) at 46°N, 112°E. None of the positive surface temperature differences in northern Asia are statistically significant.

The latitudinal-average differences in land surface

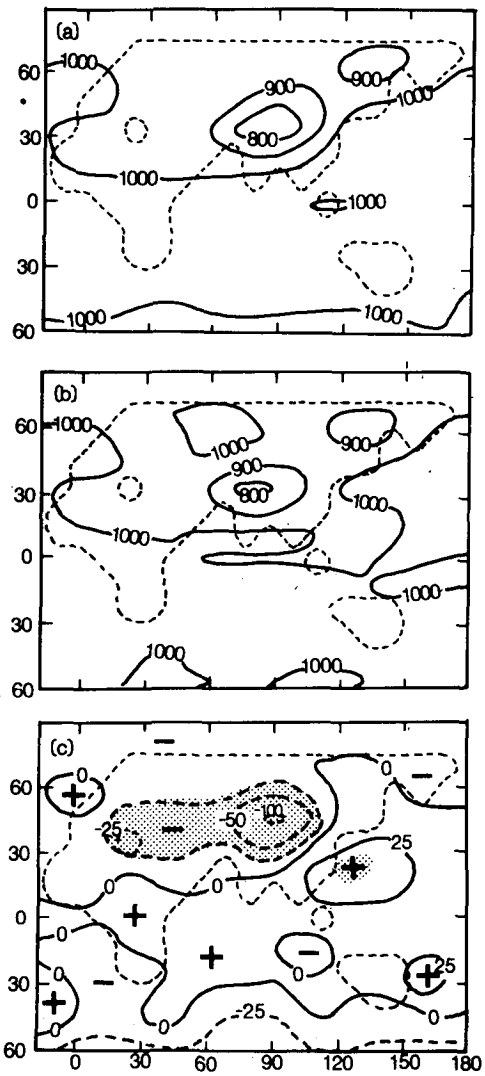

FIG. 3. Simulated 900 mb geopotential height and height differences (m) for JJA for the sector 0–180°E: (a) 9000 years B.P., (b) Modern, (c) 9000 years B.P. minus Modern. Grid points where height differences exceed two standard deviations are indicated with shading.

temperature for DJF (Fig. 2b) exceed −1.5 K (4 standard deviations) at 35 and 46°N. The DJF 9000 years B.P. surface temperature averaged over the Northern Hemisphere land is 0.7 K lower than Present (Table 2a), about 4 standard deviations.

Several factors may contribute to the relatively smaller temperature differences of DJF compared to JJA over the Northern Hemisphere land. No doubt an important factor is the relatively smaller difference of solar radiation (9000 years B.P. minus Present) for DJF compared to JJA over Northern Hemisphere land (70 to 23°N; Table 1). Temperature-albedo-snowcover feedback is not included in this model and might otherwise have helped to amplify the temperature difference. In any case, the Northern

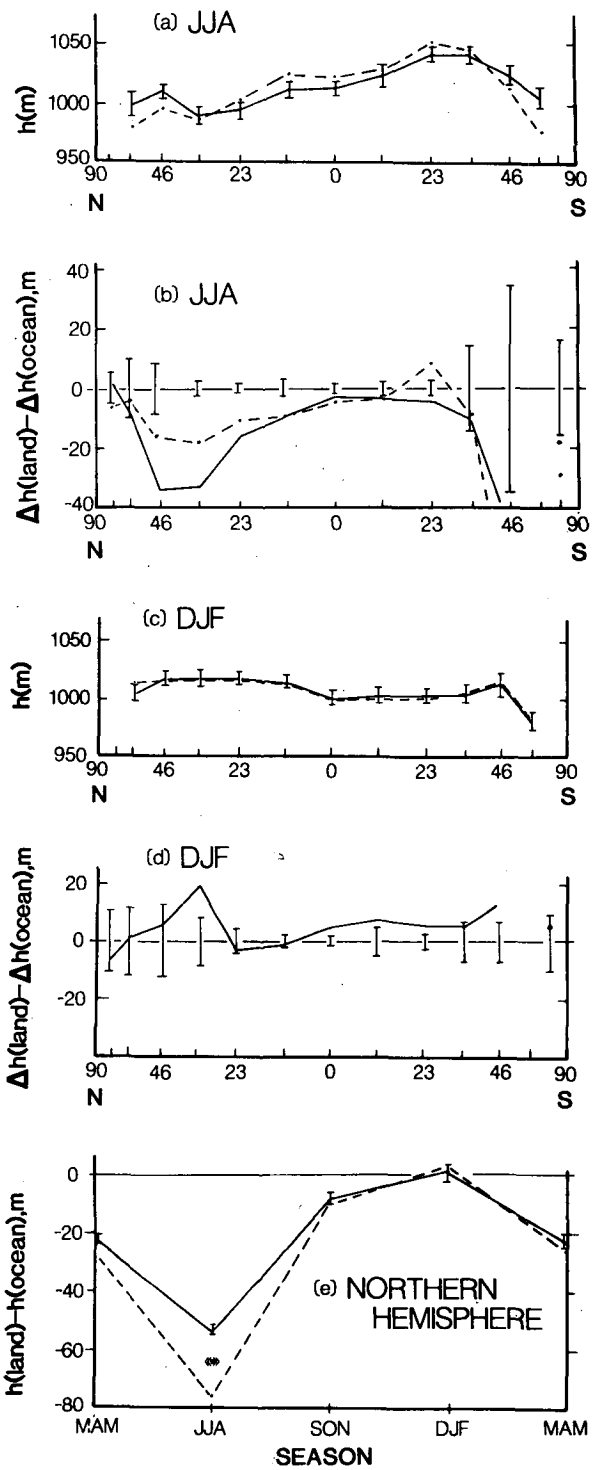

FIG. 4. Simulated 900 mb geopotential height (h, in meters) and height differences (Δh, in meters): (a) latitudinal-average height for JJA 9000 years B.P. (dashed) and for present (solid) as a function of sine of latitude; vertical bars indicate one standard deviation about the modern value. Results poleward of 70° latitude are not shown because the standard deviations of geopotential height exceed 20 m at polar latitudes. (b) Land-ocean height differences Δh(land) − Δh(ocean), JJA 9000 years B.P. minus Present, as a function of sine of latitude. Negative differences indicate

Hemisphere land temperature decreases less in DJF than it increases in JJA, and the corresponding redistribution of atmospheric mass and change of atmospheric circulation are smaller and of lower statistical significance in DJF than in JJA.

The latitudinal-average differences of 900 mb geopotential height for DJF (Fig. 4c) are less than 10 m and are less than 1 standard deviation. Nevertheless, the 900 mb heights increase slightly more over land than over ocean at most latitudes, and this indicates a weak (but not statistically significant) monsoonal response (Fig. 4d).

There are small decreases of precipitation over Northern Hemisphere land that exceed the 5% significance level (Table 2b).

c. *Annual*

The seasonal cycle of land-ocean 900 mb height differences for the Northern Hemisphere for the modern control experiment (Fig. 4e) shows a prominent lowering of height (pressure) over land in JJA. For JJA 9000 years B.P., the land-ocean height difference is increased significantly (Fig. 4e). There are no significant differences between 9000 years B.P. and the control experiment for the other seasons. This broad-scale indicator of the modified monsoon circulation for 9000 years B.P., along with the preceeding discussion of JJA and DJF differences, provides the framework for an examination of annual-average conditions.

The annual-average surface temperature, precipitation and precipitation-minus-evaporation for 9000 years B.P. (Tables 2 and 3) are appropriately weighted for the differing lengths of celestial months at 9000 years B.P. and at Present. Differences between 9000 years B.P. and Present for MAM and SON are generally smaller than the differences for JJA and DJF, consistent with the fact that solar radiation differences are also smaller in MAM and SON (Table 1), and therefore the annual-average results are generally influenced most by differences in DJF and especially JJA.

The global-average and annual-average surface temperature, precipitation and precipitation-minus-evaporation are approximately the same for 9000 years B.P. and Present (Table 2); the surface temperature is 15.9°C, the precipitation is 0.33 cm day^{-1} (~1200 mm year^{-1}). The annual-average land surface temperature is decreased slightly in the Northern Hemisphere middle latitudes (~0.5 K) but the global-average difference is near zero (Fig. 2c, Table 2a).

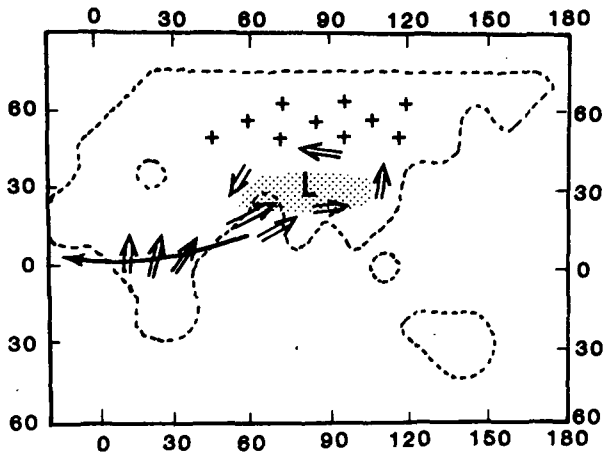

FIG. 5. Schematic of simulated temperature, pressure, wind and precipitation differences, 9000 years B.P. minus Present, for JJA: higher temperature (+), intensified monsoon low (L), stronger low-level wind (⇒), stronger upper-level wind (→), increased precipitation (shading). See Figs. 1a and 3 for details of simulated temperature and pressure differences.

The annual-average precipitation-minus-evaporation for the Northern Hemisphere land is 0.02 cm day^{-1} both for 9000 years B.P. and for the control (Table 2c). For the North African-Asian sector (Table 3b), the precipitation-minus-evaporation is increased by 0.024 cm day^{-1} (87 mm year^{-1}). The latitudinal-average difference in land $P - E$ (Fig. 6b) is positive between 11 and 35°N; at 23°N the $P - E$ increase is 0.05 cm day^{-1} (~185 mm for the year).

5. Comparison of results with and without North American ice sheet

The JJA portion of this 9000 years B.P. sensitivity experiment has been repeated with the residual North American ice sheet included as a boundary condition. At 9000 years B.P. the North American ice sheet was considerably reduced in size and especially volume as compared to its counterpart at glacial maximum (Ruddiman and McIntyre, 1981; Denton and Hughes, 1981). The ice sheet is placed at model latitudes 58, 69 and 81°N over eastern North America and covers a total of nine model gridpoints; the average thickness is ~800 m and the JJA albedo is set at 0.5. This relatively low albedo (in comparison to an albedo of 0.8 for fresh snow or ice) is used because the ice was old and may have had considerable meltwater on its surface.

The difference in the simulated climate of 9000

lower heights (lower pressure) over land than over ocean at 9000 years B.P. compared to Present. Land-ocean height difference for case with the North American ice sheet is indicated with a dashed line. There is only one land grid point at 46°S (South America) and no land grid point at 58°S. (c) same as (a) except for DJF. (d) same as (b) except for DJF. (e) 900 mb height difference between land and ocean, h(land) − h(ocean), averaged for the Northern Hemisphere, as a function of season for 9000 years B.P. (dashed), for present (solid), for JJA 9000 years B.P. with the North American ice sheet (dot in brackets). Vertical bars indicate one standard deviation about the modern value.

TABLE 3. Simulated precipitation and precipitation-minus-evaporation for June-July-August averages (a) and annual averages (b) for the land region of North Africa (30°N to equator) and the Middle East and Asia (east of 30°E and south of 40°N). This area includes 30 model grid points. Values shown are for 9000 years B.P., modern conditions, and differences. The last column in (a) refers to differences for the case with a North American ice sheet.

	9000 yr B.P. (cm day^{-1})	Modern (cm day^{-1})	Difference (cm day^{-1}) (%)	Difference with N.A. ice sheet (cm day^{-1}) (%)
a) *June-July-August*				
Precipitation	0.61	0.48	0.13 (26)	0.07 (15)
Precipitation-minus-evaporation	0.03	−0.06	0.09	0.08
b) *Annual*				
Precipitation	0.42	0.43	−0.01 (−2.5)	
Precipitation-minus-evaporation	−0.042	−0.066	0.024	

years B.P. with and without the North American ice sheet should be largest in JJA when the difference in albedo (compared to modern) is largest and when the region of the ice sheet receives its maximum solar radiation.

In the model simulations for JJA 9000 years B.P., the primary climatic impact of the ice sheet is restricted to the North American continent. At the ice sheet surface, the temperature for JJA 9000 years B.P. is 15–20 K lower than at the corresponding land surface gridpoints with no ice sheet. As a consequence, the zonal-average land surface temperature difference is changed markedly at 58 and 69°N (Fig. 2a). Over Eurasia, the pattern and order of magnitude of the temperature changes is the same as in the no-ice case (Fig. 1a); the maximum increase in JJA temperature over Asia is reduced from 5 to 4 K.

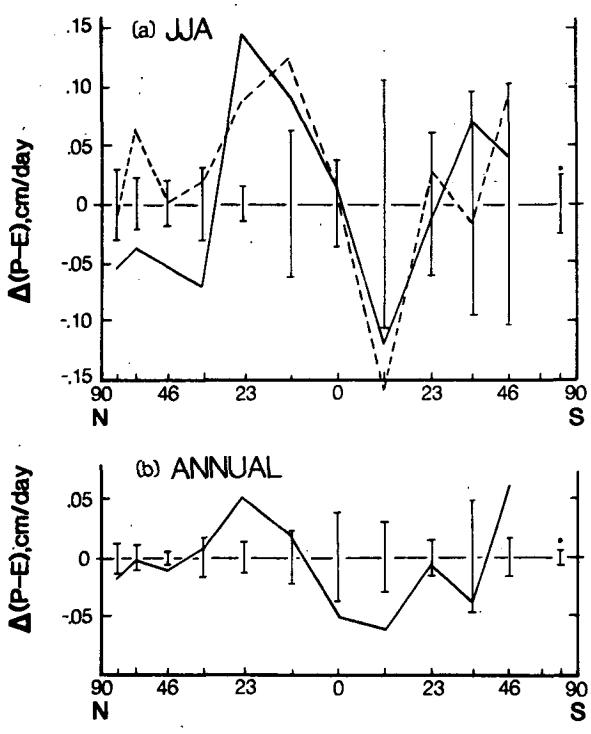

FIG. 6. Latitudinal average of simulated land precipitation-minus-evaporation difference, $\Delta(P - E)$, 9000 years B.P. minus Modern, as function of the sine of the latitude. Positive values indicate moister conditions at 9000 years B.P. compared to Present. Vertical bars indicate one standard deviation about the modern average: (a) JJA, (b) annual. $\Delta(P - E)$ for case with the North American ice sheet is indicated with dashed lines in (a). There is only one land grid point at 46°S (South America) and no land grid point at 58°S.

The Asian monsoon circulation of JJA 9000 years B.P. remains intensified (compared to modern) with the North American ice sheet included, although the intensification is reduced from the case with no ice sheet. With the ice sheet, the maximum lowering of 900 mb geopotential height is 45 m at 35°N, 79°E (the center of the monsoon low), compared to 52 m for the case with no ice sheet (Fig. 3). The zonal-average differences in 900 mb geopotential height between land and ocean show that the monsoon-like pressure response to the orbital conditions of JJA 9000 years B.P. is reduced but not eliminated by the presence of the ice sheet (Figs. 4b and 4e).

Concerning changes in the hydrologic budget, the influence of the ice sheet on the zonal-average $P - E$ rates is small (Fig. 6a). The statistically significant positive value of $\Delta(P - E)$ at 23°N is still observed, and $\Delta(P - E)$ is positive at almost all Northern Hemisphere latitudes. Evaporation is reduced (compared to modern) over the ice sheet and this accounts in large part for the increase of $\Delta(P - E)$ at high northern latitudes compared with the no-ice case. Over the North African-Asian sector, the simulated changes of P and $P - E$ for JJA with and without the North American ice sheet are similar (Table 3a).

6. Comparison with observations

Because these results are primarily a test of model sensitivity to orbital parameter variations rather than a definitive paleoclimatic simulation, only a few com-

parisons are made between the simulated and the observed paleoclimate. These comparisons are restricted to the African-Asian sector where the results are not strongly influenced by the presence or absence of the North American ice sheet. A detailed validation for the entire globe is deferred pending completion of simulation experiments with models of higher resolution.

The simulated intensification of the Northern Hemisphere summer monsoon agrees with paleoclimatic evidence in Africa and the Middle East of enlarged lakes during the early Holocene (Street and Grove, 1979). Hydrological and energy-balance equations have been used to estimate the amount of precipitation required to maintain enlarged paleolakes; when applied to lake basins and paleolakes of west and east Africa and northwest India, these balance equations yield estimates of increased precipitation (compared to modern values) of 20–100% or 100–300 mm year^{-1}, depending upon location (Street, 1979; Kutzbach, 1980). These estimates of increased precipitation are in fair agreement with other results based upon lake-level records, alluvial records and pollen records of more mesic vegetation types (Butzer *et al.*, 1972), and with the results of this 9000 years B.P. solar radiation experiment. The results of the 9000 years B.P. experiment are also of interest for studies of the cultural history of Africa and the Near East in early Holocene time (Butzer, 1971). For example, Neolithic peoples with domesticated cattle and cereals were widely distributed throughout and around the Sahara during the Holocene wet phase (Williams and Faure, 1980; Wendorf and Schild, 1980).

Lake-level records (Street and Grove, 1979) indicate that the period of enlarged paleolakes ended before 5000 years B.P.; the restriction of high lake levels to the interval 10 000–5000 years B.P. also supports the hypothesis that orbital variations are at least partly responsible for the climatic change because the solar radiation peaked around 10 000–9000 years B.P. and returned to near-modern values by 5000 years B.P. (Berger, 1978). Lake-level records for intertropical Africa and Australia show that the previous episode of high lake levels was at 30 000–25 000 years B.P. (Street and Grove, 1979), and it is significant that the seasonal radiation regimes of 30 000 and 9000 years B.P. are similar because of the ~21 000-year period of the precession cycle.

There is considerable evidence for a warmer growing season climate (compared to present) during the period 10 000–5000 years B.P. in parts of northern Eurasia. Based upon pollen and macrofossil analyses that should reflect primarily summer half-year conditions and that indicate northward shifts of 200–400 km of vegetation zones, KHotinskii (1973) concludes that a pronounced warming occurred around 10 000–9000 years B.P. in both western and eastern Siberia; this was followed by cooling ~5000 years B.P. The warming occurred somewhat later (~8000 years B.P.) and more gradually in eastern Europe, but was also followed by cooling ~5000 years B.P.

7. Conclusions

In addition to the inherent limitations of a low-resolution model, this particular model employs various simplified parameterizations of physical processes that may have produced unrealistic features of the simulated climate. Because of these model limitations, our results should be compared with results from models with higher resolution or improved physics and this work is underway using the Community Climate Model of the National Center for Atmospheric Research. Although the general features of the 9000 years B.P. climate are probably simulated correctly by this model, improved models are required for more detailed and accurate paleoclimatic simulations.

Strong evidence for important feedback relationships between ocean, atmosphere and ice sheets on the time-scale of the orbital parameter variations (Ruddiman and McIntyre, 1981) has been ignored in this experiment, as have possible CO_2 feedbacks (Thompson and Schneider, 1981). A coupled atmosphere-ocean model could also be used to aid in the evaluation of the climatic response to the altered seasonal solar radiation cycle at 9000 years B.P.

Nevertheless, the results presented by Kutzbach (1981) are supported by this more detailed summary of the simulated 9000 years B.P. climate both with and without the North American ice sheet. These results suggest that the solar radiation changes associated with orbital parameter variations are at least partly responsible for changes of the climate of the early Holocene. The changes are large and statistically significant for certain regions and seasons, and indicate a strengthened Northern Hemisphere summer monsoon over the African-Eurasian land mass at 9000 years B.P.

Acknowledgments. Research grants to the University of Wisconsin-Madison from the National Science Foundation's Climate Dynamics Program (NSF Grants ATM79-16443, ATM79-26039 and ATM79-11996) supported this work. The authors thank P. Guetter for performing the computations, E. Hopkins for the algorithm used to calculate the solar radiation for 9000 years B.P. in initial calculations, and the reviewers for comments and suggestions that led to revisions of the manuscript. The computations were made at the National Center for Atmospheric Research (NCAR), which is sponsored by the National Science Foundation, with a computing grant from the NCAR Computing Facility.

J.E.K. acknowledges with thanks the opportunity

to present this paper as the Richard Foster Flint Lecture in Quaternary Geology at the Department of Geology and Geophysics of Yale University, New Haven, CT on 24 March 1982.

REFERENCES

Berger, A. L., 1978: Long-term variations of caloric solar radiation resulting from the earth's orbital elements. *Quat. Res.*, **9**, 139–167.

Bernard, E. A., 1962: Théorie astronomique des pluviaux et interpluviaux du Quaternaire African. *Acad. Roy. Sci. Outre-Mer (Brussels), Classe Sci., Tech. Mémo. in 8°*, **12**, No. 1., 232 pp.

Bryson, R. A., W. M. Wendland, J. D. Ives and J. T. Andrews, 1969: Radiocarbon isochrones of the disintegration of the Laurentide Ice Sheet. *Arctic Alpine Res.*, **1**, 1–14.

Butzer, K. W., 1971: *Environment and Archeology: An Ecological Approach to Prehistory*. Aldine-Atherton, 703 pp.

——, G. L. Isaac, J. L. Richardson and C. Washbourn-Kamau, 1972: Radiocarbon dating of East African lake levels. *Science*, **175**, 1069–1076.

Chervin, R. M., J. E. Kutzbach, D. D. Houghton and R. G. Gallimore, 1980: Response of the NCAR general circulation model to prescribed changes in ocean surface temperature. Part II: Midlatitude and subtropical changes. *J. Atmos. Sci.*, **37**, 308–332.

CLIMAP Project Members, 1976: The surface of the Ice-Age Earth. *Science*, **191**, 1131–1136.

Denton, G. H., and T. J. Hughes, Eds., 1981: *The Last Great Ice Sheets*. Wiley, 484 pp., 28 folded maps.

Gates, W. L., 1976a: Modeling the Ice-Age climate. *Science*, **191**, 1138–1144.

——, 1976b: The numerical simulation of Ice-Age climate with a global general circulation model. *J. Atmos. Sci.*, **33**, 1844–1873.

Hays, J. D., J. Imbrie and N. J. Shackleton, 1976: Variations in the Earth's orbit: Pacemaker of the ice ages. *Science*, **194**, 1121–1132.

Imbrie, J., and K. P. Imbrie, 1979: *Ice Ages: Solving the Mystery*. Enslow Publishers, 224 pp.

——, and J. Z. Imbrie, 1980: Modeling the climatic response to orbital variations. *Science*, **207**, 943–953.

Khotinskii, N. A., 1973: Transkontinental'naia Korreliatsiia etapov istorii rastitel'nosti i klimata severnogo; Evrazii v. Golotsene. *Probl. Palinologii Tr. III Mezhdun. Palinolog. Konf.*, M. I. Neishtadt, Ed., Moscow, Nauka, 116–123. [English translation by G. M. Peterson available from Center for Climatic Research, 1225 W. Dayton, Madison, WI 53706].

Kutzbach, J. E., 1980: Estimates of past climate at Paleolake Chad, North Africa, based on a hydrological and energy-balance model. *Quat. Res.*, **14**, 210–223.

——, 1981: Monsoon climate of the early Holocene: climatic experiment using the Earth's orbital parameters for 9000 years ago. *Science*, **214**, 59–61.

Manabe, S., and D. G. Hahn, 1977: Simulation of the tropical climate of an Ice Age. *J. Geophys. Res.*, **82**, 3889–3911.

Mason, B. J., 1976: Towards the understanding and prediction of climatic variations. *Quart. J. Roy. Meteor. Soc.*, **102**, 473–498.

Milankovitch, M., 1941: *Canon of Insolation and the Ice-Age Problem. K. Serb. Akad. Geogr.*, Spec. Publ. No. 132, 484 pp. [Translated by Israel Program for Scientific Translations, Jerusalem, 1969, U.S. Dept. of Commerce].

Otto-Bliesner, B. L., G. W. Branstator and D. D. Houghton, 1982: A global low-order spectral general circulation model. Part I: Formulation and seasonal climatology. *J. Atmos. Sci.*, **39**, 929–948.

Ruddiman, W. F., and A. McIntyre, 1973: Time-transgressive deglacial retreat of polar waters from the North Atlantic. *Quat. Res.*, **3**, 117–130.

——, and ——, 1981: Oceanic mechanisms for amplification of the 23,000-year ice-volume cycle. *Science*, **212**, 617–627.

Schneider, S. H., and S. L. Thompson, 1979: Ice ages and orbital variations: some simple theory and modeling. *Quat. Res.*, **12**, 188–203.

Street, F. A., 1979: Late Quaternary precipitation estimates for the Ziway-Shala Basin, Southern Ethiopia. *Palaeoecology Africa*, **11**, 135–143.

——, and A. T. Grove, 1979: Global maps of lake-level fluctuations since 30,000 yr B.P. *Quat. Res.*, **12**, 83–118.

Suarez, M. J., and I. M. Held, 1976: Modeling climatic response to orbital parameter variations. *Nature*, **263**, 46–47.

——, and ——, 1979: The sensitivity of an energy balance climate model to variations in the orbital parameters. *J. Geophys. Res.*, **84**, 4825–4836.

Thompson, S. L., and S. H. Schneider, 1981: Carbon dioxide and climate: ice and ocean. *Nature*, **290**, 9–10.

Vernekar, A. D., 1972: *Long-Period Global Variations of Incoming Radiation. Meteor. Monogr.*, No. 34, Amer. Meteor. Soc., 21 pp. + tables.

Wendorf, F., and R. Schild, 1980: *Prehistory of the Eastern Sahara*. Academic Press, 414 pp.

Wetherald, R. T., and S. Manabe, 1975: The effects of changing the solar constant on the climate of a general circulation model. *J. Atmos. Sci.*, **32**, 2044–2059.

Williams, J., R. G. Barry and W. M. Washington, 1974: Simulation of the atmospheric circulation using the NCAR global circulation model with Ice Age boundary conditions. *J. Appl. Meteor.*, **13**, 305–317.

Williams, M. A. J., and M. Faure, Eds., 1980: *The Sahara and the Nile: Quaternary Environments and Prehistoric Occupation in Northern Africa*. Balkema, Rotterdam [U.S. distribution, Merrimack Book Service, Salem, NJ], 608 pp.

Zeuner, F. E., 1959: *The Pleistocene Period–Its Climate, Chronology and Faunal Successions*. Hutchinson, London, 447 pp.